Miniaturization of EBG Structures using Embedded Capacitance Material

O.V.Tereshchenko [#1], F. J. K. Buesink [#2], F. B. J. Leferink [*#3]
[#]EEMCS, Telecommunication engineering group,
University of Twente,
Carre, C2116, PO Box 217, 7500AE, Enschede, The Netherlands
[1]o.tereshchenko@ewi.utwente.nl
[*]Thales Nederland B.V.
P.O. Box 42, 7550 GD Hengelo, the Netherlands

***Abstract*—The effect of embedded capacitance material on the size reduction and filtering performance of electromagnetic band gap (EBG) structures etched on a power plane has been investigated. Due to the high permittivity of the embedded material the effective band shifts to much lower frequencies. The impact of these EBG structures on resonances in power distribution network has been modeled using an equivalent circuit model, and simulated using a SPICE circuit simulator. The model and simulation results has been compared with measurement results. The effect of EBG on common mode radiation was evaluated.**

Keywords - EMC; EBG, resonances, PDN, SSN noise

I. INTRODUCTION

The fast signal rise times of digital logic circuits imply fast current surges in the devices' power supply lines. If many outputs are switched simultaneously, such as in a synchronous system, these transient currents flow in the power distribution network, causing voltage drops due to the finite impedance of the power and ground planes [1]. At high frequencies the power-ground planes start to resonate and the power distribution network shows large impedance which leads to voltage fluctuations towards the connected devices. This phenomena is also known as simultaneous switching noise (SSN) 1, causing Signal Integrity (SI) and Power Integrity (PI) problems. The noise developed in the reference or ground plane results also in antenna currents in connected cables leading to Electromagnetic Interference (EMI) 0. Several methods to decrease the impedance in the power distribution network have been used in the last decade, including the use of embedded decoupling capacitors [1]- [3]. Another way is to implement Electromagnetic Band Gap structures (EBG) 0-[8]. However, EBGs can mitigate noise only in the GHz range due to the limited size. In this paper the combination of EBG structures with embedded capacitance material has been investigated. This solution leads to miniaturization of EBGs and results in large and wideband suppression of power/ground noise. The filtering performance of EBG structures on embedded capacitor material was investigated both by measurements and simulations.

II. EQUIVALENT CIRCUIT MODEL OF EBG STRUCTURE

Power distribution is generally achieved by low impedance conductors such as power and ground planes. In conventional design approach the power plane mirrors the ground plane and creates a transmission line sandwich which behaves as an electromagnetic resonant cavity. Transient current flows between power and ground plane and creates a noise voltage across the impedance of the plane causing noise voltages in the ground plane. This noise voltage creates common mode current emission either by direct radiation from the board or by coupling to connected cables. In addition, a transients current flowing around the loop formed by power and ground planes makes an efficient loop antenna. The frequency of the power plane resonance is determined by its physical size and dielectric constant of the insulator 0. The parallel plane resonances can also be represented as an interaction of low loss inductances with low loss capacitances. Via this equivalent circuit model the interaction of parasitic effects can be implemented easily. The most troublesome interactions are usually the parasitic inductance towards the integrated circuit (IC) die capacitance and the parasitic inductance to the PCB, i.e. the interconnects.

Electromagnetic band gap (EBG) structures can reduce the resonances in PDN and decrease common mode noise 0. The Power Distribution Network (PDN) employing EBG structures becomes a low-pass filter reducing unwanted resonances and radiated electromagnetic fields. By implementing EBG in PDN its symmetry is changed drastically towards an asymmetric design by using smaller power patches over the large ground plane. The beneficial effect of asymmetry on reduced EMI has been shown in [9]-[12]. The EBG patches are interconnected by thin traces. The resulting structure acts as a low-pass EBG filter. The exact frequency characteristic is determined by parameters of the EBG structures. To model the behaviour of 2-dimensional EBG structures an equivalent circuit have been used and a SPICE circuit simulator was used to simulate the effect [13]. The first experimental board (Figure 1 and 2) was built on a standard FR4 substrate. This board contains several fragments of EBG structures, each of them has different size of patch and different trace length (Table I). The meander is used as inductive decoupling, while the EBG patch itself can be considered as a capacitor. The SPICE model considers thus

both patches and traces above the ground reference plane modelled as loss-less transmission lines.

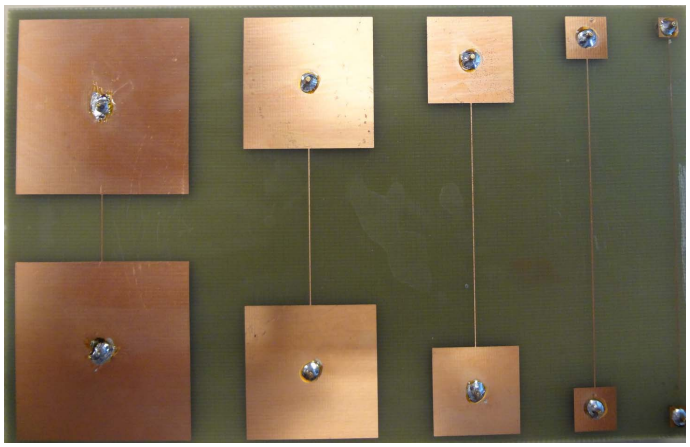

Fig. 1. Five Sets of Interconnected Power Islands, over the bottom ground plane, acting as an low-pass EBG

TABLE I. DIMENSIONS OF ISLANDS AND TRACE LENGTHS

Set	Patch size	Connecting Trace Length
-	mm	mm
1	40x40	15
2	30x30	35
3	20x20	55
4	10x10	75
5	5x5	85

To model the effect of noise voltage in the ground reference plane, the effective inductance was obtained from the coupled flux [14].

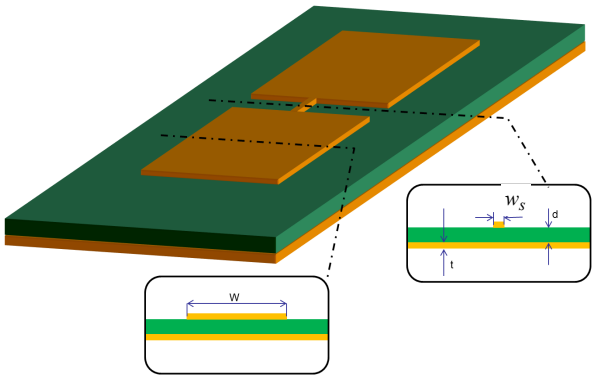

Fig. 2. Cross Sectional View of Power Patches and Trace

$$H(r) = \frac{tracecurrent}{contourcircumference} = \frac{I}{2(\pi r + w_s + t)} \quad (1)$$

$$B(r) = \frac{\mu_0 I}{2(\pi r + w_s + t)} \quad (2)$$

While Equation 2 calculates the partial magnetic induction as a result of the current in the trace, the same equation was used using the width of the power patch, w, instead of the trace width, w_s, to calculate the field resulting from the current in the patch.

$$\Phi = \int_{r=0}^{r=d} B(r)\partial r \quad (3)$$

Equations 4 and 5 show the results for the power patches and ground reference plane respectively. The results for many other geometries were described in [14]

$$L_{patch}PUL = \frac{\Phi}{I} = \frac{\mu_0}{2\pi} \cdot \ln\left[\frac{\pi \cdot d}{W + t} + 1\right] \quad (4)$$

$$L_{ground}PUL = \frac{\Phi}{I} = \frac{\mu_0}{2\pi} \cdot \ln\left[\frac{\pi \cdot d}{W_{Ref} + t} + 1\right] \quad (5)$$

Each trace was modelled as L - C sections shorter than $\frac{\lambda}{2\pi}$ where λ is the wavelength of the highest excitation frequency. Each patch was meshed into squares with dimensions smaller than $\frac{\lambda}{2\pi}$. $F_{max} = 3GHz$ was considered as the highest frequency in this analyses, the shortest wavelength was given by Equation 6. $\frac{\lambda_{min,Patch}}{2\pi} = \frac{1}{F_{max}\ \tau_{PD}} = 0.05m$ (6)

To model the source and load connector in the middle of the patch, each side of a patch had an even number of squares. Each patch was meshed as shown in Figure 3. The edges of each square in Figure 3 were replaced by small inductors and the nodes on each corner by small capacitors. The same process was used for the ground reference plane. All node capacitors were "vertical". The SPICE model for a patch is a matrix of capacitors interconnected by inductances as shown in Figure 7. Each capacitor was connected to the triangular ground symbol, provisionally showing the reference plane as an ideal conductor with zero resistance and inductance in order not to complicate the picture too much. The final model included also the reference plane as a grid of inductances where the capacitances were connected to the nodes in this grid. The actual wavelength, needed to calculate the maximum section or mesh dimension, depends on the propagation delay, τ_{PD}, of the transmission line under consideration.

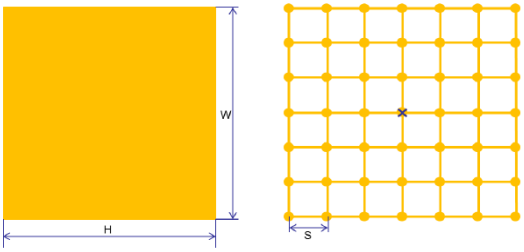

Fig. 3. Subdivision of the Largest Power Island

The effective permittivity depends on the geometry of the transmission line. For the patches, which are much wider than twice the base material thickness, d, the effective permittivity was calculated using Equation 7.

$$\epsilon_{eff-Patch} = \frac{\epsilon_r + 1}{2} + \frac{\frac{\epsilon_r - 1}{2}}{sqrt\frac{10 \cdot d}{W} + 1} \quad (7)$$

In which W is the width of the patch and d the thickness of the base material as defined in Figure 2. The base material permittivity, ε_r were found from the parallel plate capacitor expression, Equation 8, resulting in Equation 9.

$$C_{pplate} = \frac{Area_{cap}\varepsilon_0\varepsilon_r}{d} \quad (8) \qquad \varepsilon_r = \frac{C_{pplate}d}{Area_{cap}\varepsilon_0} \quad (9)$$

$$\varepsilon_{eff\ \ Patch} = 4.2 \text{ With } \varepsilon_0 = 8.85\ \ 10^{-12}\frac{F}{m}, \quad (10)$$

the measured value $C_{pplate} = 40pF$ for the 40 x 40mm patch with $Area_{cap} = 1.6\ \ 10^{-3}m^2$, the permittivity of the base material was found as $\varepsilon_r = 4.5$. Equation 10, the effective permittivity for the patch, was evaluated as $\varepsilon_{eff\ \ Patch} = 4.2$. The propagation delay for the patch area was defined as then $\tau_{PD} = 6.9\frac{ns}{m}$. The maximum side of each mesh (S in Figure 3) then was $\frac{\lambda_{min,Patch}}{2\pi} = 8mm$. For the largest patch on our board (#1 in Table I) with dimensions W x H = 40 x 40mm, each side got hence at least 5 squares. But the middle of the patch should also be available in the model. That requires an even number of meshes. So at least six meshes, S = 6:7 mm, on each side for the patch as shown in Figure 3. This model had 49 nodes per power patch. For a total patch capacitance of $C_{patch} = 40pF$ this means each capacitor in the model was $C_{node,patch} = 0.8pF$.

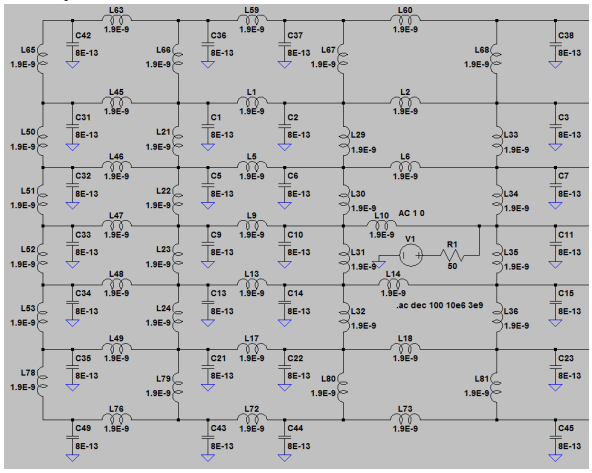

Fig. 4. SPICE Model for 1 Power Patch (Partial View)

To validate the model measurements of the attenuation S21 were performed. The measurement and simulation results are plotted in Fig. 5. These graphs illustrate that the measurements match simulations and the proposed model has sufficient accuracy. The calculated results are generally consistent with the experimental data. The band gap frequencies are shifted to a higher value. It can be related to the frequency dependencies of the FR-4 material, which were neglected in the SPICE models and to the couplings outside the EBG structures, which were neglected in the SPICE models. The calculated stop bands are reasonably accurate.

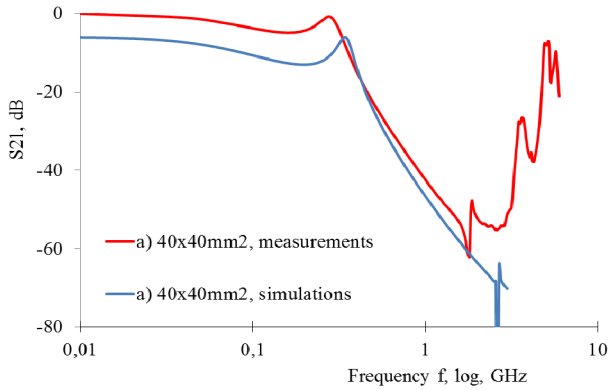

Fig. 5: Measurements and simulation of transfer function of EBG structure

Most EBG are mitigating noise in a limited bandwidth (GHz range). To improve the filtering performance of EBG without increasing the size of the structure, EBG on high k substrate were manufactured.

III. EBG STRUCTURE ON HIGH-k MATERIAL

Four experimental boards were designed to demonstrate the influence of the substrate material, shape, length, inductance of meander line, size and capacitance of patches on resonances in power plane and common mode radiation (Figure 6). Board 1 and 2 were designed on EURO-card printed circuit boards (100 × 160 mm2). The dielectric of the PCB was FR4 with relative dielectric constant of 4.7. Board 3 and 4 were designed on embedded capacitor material with dielectric constant 22, which is almost 4 times higher than permittivity of FR4 material. Board 1 and 3 had the same design configuration. The first structure (board 1-a) represented conventional power plane which mirrors the ground plane creating a cavity. The geometries of three other arrays (board 1-b-c-d and board 2- b-c-d) were as follows. The size of each individual patch was 30 × 30 mm2. Inductance of meander for the case 1-b) and 2-b) is 453 nH, EBG fragments 1-c), 2-c), 1-d), 2-d) have equal inductance of the interconnecting line which is 325 nH. All interconnection traces were 0.5 mm wide.

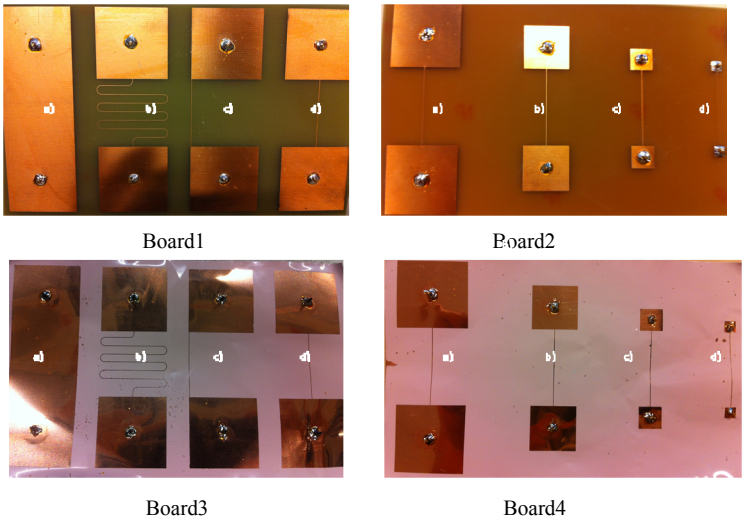

Fig. 6 Set of EBG structures etched on high-k material and FR4 substrates.

Board 2 and 4 were designed to estimate the influence of the size of individual patch of EBG on radiated emission. These 2 boards also had the same design configuration. Dimensions of the island for each EBG fragment are listed in Table II. All interconnection traces were 0.5 mm wide and 35 mm long.
The transfer function of the boards shown in Figure 6 was measured and plotted in Fig.7 and 8. The graph demonstrate that the EBG reduces resonances in the PDN. Significant noise reduction is achieved by combination of EBG and high capacitance substrate in comparison with standard power plane.

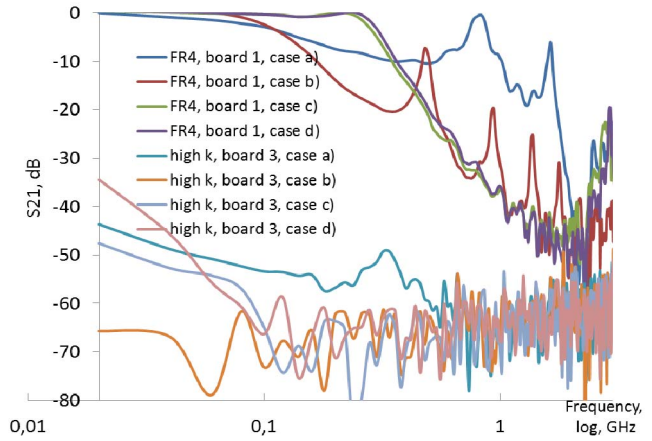

Fig. 7: S21 of EBG with different meander lines on FR4 and high-k, board 1

Measurement results of S21 of the board with different size of the patches are plotted on Figure 8 which demonstrates that EBG etched on high dielectric material show better performance at low frequencies. The EBG with the smallest patch size (5x5mm) etched on high-k substrate shows 5 dB better attenuation than EBG on FR4 (30x30). This demonstrates the fact that combination of EBG structure and embedded capacitance material could be used to suppress SSN noise in high speed electronics

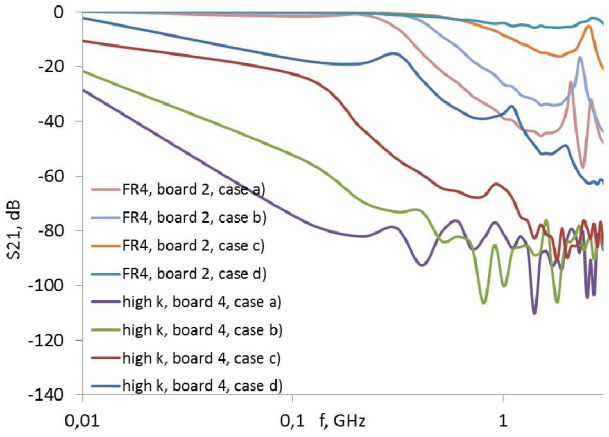

Fig. 8: Attenuation of EBG with different patches on FR4 and high-*k*, board 2

TABLE II DIMENSIONS OF ISLANDS AND TRACE LENGTHS

Set	Patch size
-	mm
1	30x30
2	20x20
3	10x10
4	5x5

IV. CURRENT CLAMP MEASUREMENTS

One of the most important immunity tests is assessment of common mode radiation which can be realized by measuring of common mode currents on the cables. The radiation from the cables is directly proportional to the common-mode current on that cable. Common mode emission can be modelled as a dipole, or monopole antenna (the cable) driven by a noise voltage (the ground voltage). For a short dipole antenna of length l, the magnitude of electric field strength measured, in the far field, at a distance r from the source is

$$E = \frac{4\pi \times 10^{-7} (flI_{cm}) \sin\theta}{r}, \qquad (11)$$

where E is in volts/meter, f is in hertz, I is the common-mode current on the cable (antenna) in amperes, l and r are in meters, and θ is the angle from the axis of the antenna that the observation is made. The maximum field strength will occur perpendicular to the axis of the antenna where $\theta = 90°$. The measurements of common mode current were performed with Absorbing Clamp EM 101 and PNAL Network Analyzer (NA) Agilent technologies N5230A. The current clamp is an RF current clamp, having inductive and capacitive coupling and allowing the induction of large currents on cables in the frequency range of 0.15 MHz to 1 GHz. The absorbing clamp is both a current probe and an «antenna impedance» formed by a number of ferrite ring cores arranged in a row that surround the cable of the equipment under the test (EUT). Some of these ring cores are part of the current transformer. The output voltage of this current transformer is taken to the measuring receiver via an internal RF cable also loaded by ferrite rings. With power cables, the measurement result is not affected by the magnitude of the current since the currents of the forward and return leads cancel each other out. The clamp consists of a two-part plastic case that can be opened. Each part includes a set of ferrite ring core halves. The halves are arranged in spring-loaded holding devices to form a channel to surround the cable of the EUT to be inserted. By closing the upper part of the plastic case, the magnetic loop around the cable is completed. Practical eccentric catches provide the necessary contact pressure.

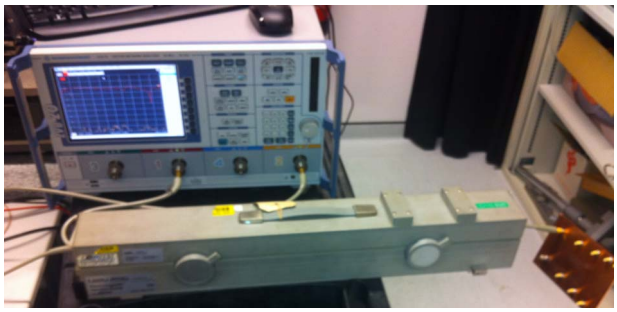

Fig.9 Set up for common mode measurements

The major advantage of the clamp is the highly repeatable and comparable common mode current measurements, compared to common mode measurements using current probe only . Fig.9 shows the measurement set up used for our experiments. The measured cable (1 m length) was placed on a non-conducting surface (test table) so that it was at least 40 cm away from a conductive floor or wall. It was connected to port 2 of the NA and stretched out over the length of absorbing clamp. Then different board configurations with 50Ohm load termination were connected to the cable. The current transformer was facing the equipment under of the test (EUT) . The generator in the network analyser was feeding the inner circuits with a test signal:

- Case a) standard power plane,
- Case b) EBG structured power plane
- Case c) EBG structured power plane on high k substrate

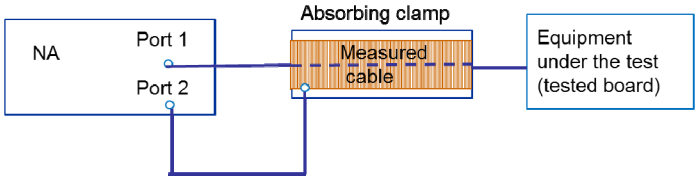

Fig.10 Common mode measurements setup scheme

Another port of NA was connected to absorbing clamp. Via the absorbing clamp the cable acts as an antenna tuned at all frequencies. The clamp induces a current on a cable by using inductive and capacitive coupling at the same time. Inductive coupling is realised by transformer having a one turn primary circuit which uses the clamp`s ferrite tube of 60 cm length as magnetic core. The mechanism of capacitive coupling between the cable under the test and the primary turn (semi cylinder of a metal foil in the groove of the clamp) is as follows : the resistance in the impedance of the primary turn enhances the directional effect and diminishes the influence of the load at the "back side" of the clamp. A ferrite absorber provided in the clamp surrounds the power cable and acts as resistance for the high-frequency RFI power. The incoming current is measured at the absorber input by using a current transformer and an EMI measuring receiver. Since there is no matching between the disturbance source, the cable, and the absorber in this setup, the clamp is slid along the cable to obtain maximum current.

Fig.11 Electromagnetic Absorbing Clamp

Measurements of these 4 experimental boards demonstrated that the length of the meander has no influence on common mode current (Fig.6) and the standard PDN design approach, which corresponds to board 1 a), shows the highest emission level.

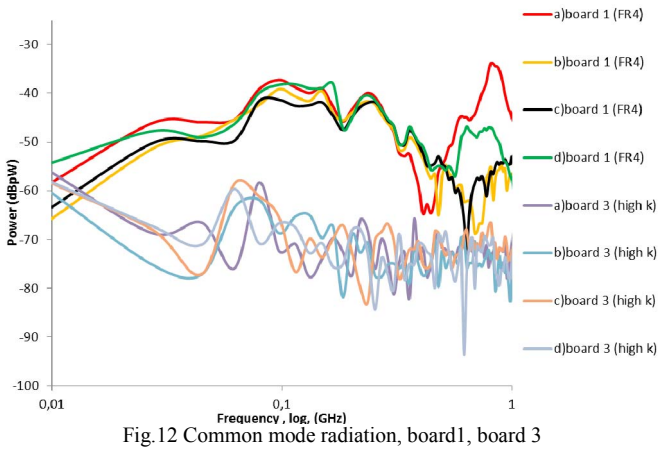

Fig.12 Common mode radiation, board1, board 3

It is possible to achieve almost 35 dB difference in radiated emission implementing EBG on high permittivity substrate. Fig. 6 shows the measured common mode currents for board 2 and board 4. The measurements demonstrate that even with the smallest patch of EBG on high permittivity substrate it is possible to achieve better common mode noise mitigation than with standard power plane solution.

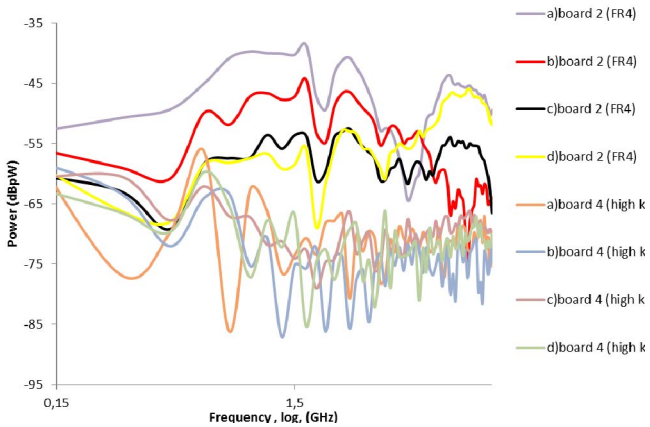

Fig.13 Common mode radiation, board 2, board 4

All measured amplitudes are written in terms off dBpW, according to the convention that the absorbing clamp is measuring the radiated power.

V. CONCLUSION

Implementation of Electromagnetic Band Gap (EBG) structures reduces unwanted resonances in Power Distribution Network (PDN). This leads to mitigation of common mode current and therefore reduced common mode radiation. By modelling in SPICE design parameters of EBG structures, different transfer function were achieved. Measurements show that created model is valid and that the EBG structures are acting as low-pass filter.

The high *k* material can be used as a substrate to miniaturize the EBG structures. Moreover combination of EBG and high *k* embedded material substrate leads to better filtering performance of EBG even at lower frequencies. Measurements of transfer function and common mode current of EBG on high *k* material proved that its possible to achieve almost 40 dB difference in common mode radiated emission comparing with standard PDN solution.

REFERENCE

[1] Howard Johnson, Martin Graham "High-Speed Digital Design, A Handbook of Black Magic" Prentic Hall PTR, Upper Saddle River, NJ07458, ISBN 0-13-395724-1

[2] S. Van de Berghe, F. Olyslager, D. De Zutter, J. De Moerloose, and W.Temmermann, "Study of the ground bounce caused by power plane resonances," IEEE Trans. Electromagn. Compat., vol. 40, pp. 111–119,May 1998.G.

[3] O.V.Tereshchenko, F. J. K. Buesink, F. B. J. Leferink "Reduction of Power Plane Resonances using EBG Structures to Decrease Common Mode Current", Asia-Pacific Symposium on Electromagnetic Compatibility, Singapore, 2012

[4] H.W. Ott "Decoupling" http://www.hottconsultants.com/techtips/decoupling.html#zycon

[5] D. Sievenpiper, L. Zhang, Romulo F. J.Broas, E.Yablonovitch, "High-Impedance Electromagnetic Surfaces with a Forbidden Frequency Band",Microwave Theory and Techniques, IEEE Transactions, 1998

[6] Jong Hwa Kwon; Dong Uk Sim; Sang Il Kwak; Jong Gwan Yook; "Novel Electromagnetic Bandgap Array Structure on Power Distribution Network for Suppressing Simultaneous Switching Noise and Minimizing Effects on High-Speed Signals "Electromagnetic Compatibility, IEEE Transactions on 2010

[7] Arghiani, M. "Simultaneous switching noise (SSN) suppression with a new Embedded Uniplanar Compact Electromagnetic Bandgap (EUCEBG) structure ", APMC, 2010

[8] Ting-Kuang Wang; Tzu-Wei Han; Tzong-Lin Wu; "A Novel Power/Ground Layer Using Artificial Substrate EBG for Simultaneously Switching Noise Suppression", IEEE Transactions on Microwave Theory and Techniques, 2008

[9] Frank Leferink, Signal to noise transformation, the key to EMC, IEEE Symposium on EMC, Chicago(USA) 1994, pp. 462-467

[10] Frank Leferink, Reduction of Radiated Electromagnetic Fields by Creation of Geometrical Asymmetry, PhD Thesis University of Twente, 21 nov. 2001

[11] Frank Leferink, Wim C. van Etten, The Beneficial Effect of Removing Power Planes on the Radiated Emission of Printed Circuit Boards, EMC Europe 2004, Eindhoven, pp. 367-371,

[12] Frank Leferink, Wim C. van Etten, Reduction of Radiated Electromagnetic Fields by Removing Power Planes, IEEE International Symposium on EMC, Santa Clara, pp. 226-230,

[13] O.V.Tereshchenko, F. J. K. Buesink, F. B. J. Leferink "EBG Structures on High Permittivity Substrate to Reduce Noise in Power Distribution Network", IEEE EMC Simposium, Pittsburgh, 2012

[14] F.B.J. Leferink "Inductance Calculations; Methods and Equations" IEEE Symposium on EMC, Atlanta(USA) 1995